Functionalized molecules studied by STM: motion, switching and reactivity

2008 J. Phys.: Condens. Matter 20 053001

(http://iopscience.iop.org/0953-8984/20/5/053001)

IOP PUBLISHING JOURNAL OF PHYSICS: CONDENSED MATTER

J. Phys.: Condens. Matter **20** (2008) 053001 (19pp) doi:10.1088/0953-8984/20/05/053001

TOPICAL REVIEW

Functionalized molecules studied by STM: motion, switching and reactivity

Leonhard Grill

Institut für Experimentalphysik, Freie Universität Berlin, Arnimallee 14, 14195 Berlin, Germany

E-mail: leonhard.grill@physik.fu-berlin.de

Received 2 November 2007, in final form 5 December 2007
Published 8 January 2008
Online at stacks.iop.org/JPhysCM/20/053001

Abstract

Functionalized molecules represent the central issue of molecular nanotechnology. Scanning tunnelling microscopy (STM) is a powerful method to investigate such molecules, because it allows us to image them with sub-molecular resolution when adsorbed on a surface and can be used at the same time as a tool to manipulate single molecules in a controlled way. Such studies permit deep insight into the conformational, mechanical and electronic structure and thus functionalities of the molecules. In this review, recent experiments on specially designed molecules, acting as model systems for molecular nanotechnology, are reviewed. The presented studies focus on key functionalities: lateral rolling and hopping motion on a supporting surface, the switching behaviour of azobenzene derivatives by using the STM tip and the controlled reactivity of molecular side groups, which enable the formation of covalently bound molecular nanoarchitectures.

(Some figures in this article are in colour only in the electronic version)

Contents

1. Introduction

The fascinating vision of molecular nanotechnology lies in the use of single molecules as machines or devices and the controlled assembly of molecular matter at the nanometre scale (nanomanufacturing). The possibility to manipulate and control things on a small scale was first introduced by Richard Feynman in his famous 1959 speech 'There's plenty of room at the bottom' [1]. Resulting applications, like electronic circuits, sensors or nanomachines, would, due to their small dimensions, open the door to completely new technologies, with advantages in cost, operation speed (efficiency) and power dissipation. In contrast to top-down approaches (e.g. by improving lithographic techniques), the use of molecules reveals several important advantages:

(1) *Molecules have nanoscale dimensions by nature*: thus, the use of single molecules automatically leads to structural dimensions at the atomic scale. The top-down miniaturization of existing applications and devices requires fundamental improvements of conventional fabrication techniques, which are limited.
(2) *Molecular recognition*: intermolecular interactions can be used to grow molecular nanostructures. Molecules are known to self-organize according to their chemical

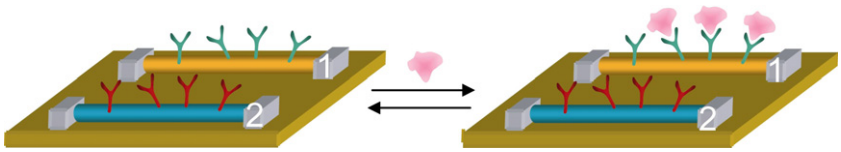

Figure 1.1. Principle of biosensors. Two nanowire devices (1 and 2) are modified with different (1, green; 2, red) antibody receptors. A cancer marker protein that binds specifically to its receptor (on nanowire 1) will produce a conductance change characteristic of the surface charge of the protein only on nanowire 1. From Lieber and co-workers. Reproduced with permission from [5]. Copyright (2005) Nature Publishing Group.

properties and to self-assemble in topologies that reflect the interactions between them. By controlling the chemistry of the involved molecules, various structures of different size and shapes can be produced.

(3) *Capabilities of organic chemistry*: by choosing the structure and composition of a molecule, chemical synthesis can be used to produce molecules of precisely defined properties.

(4) *Functions*: molecules can have specific functions, for instance switching between different states (of characteristic optical, magnetic and electronic properties). In fact, this is a fundamental concept in nature, where many molecules have multiple stable isomers.

These characteristics make molecules very suitable for applications in the field of molecular nanotechnology, which divides into several sub-topics. Some main issues are discussed in the following.

The high selectivity caused by molecular recognition is of great interest for the development of so-called intelligent materials, where molecules act as highly sensitive detectors for another specific type of molecule or nanoparticle. A famous example in this context is the so-called artificial nose, where differently coated cantilevers are used to characterize vapours [2]. Intense research activities in this field are focusing on biosensors [3, 4], which contain biological components like proteins, enzymes or antibodies that bind (or do not bind) selectively to a substance of interest. This concept is illustrated in figure 1.1, where two nanowires are equipped with different receptors [5]. After exposing the device to specific cancer marker proteins, only one nanowire is modified while the other one remains intact. Additional to the biologically sensitive part, such sensors require the detection of a signal related to the chemical processes. In figure 1.1, this is achieved by a change in the conductance properties of nanowire 1, while nanowire 2 remains unchanged. Thus, proteins are detected electrically with extremely high sensitivity, as only very small quantities of the detected substance are required. Furthermore, the process is highly selective, because the receptors exclusively bind to the proteins in question. Additionally to the electric detection, an important class of biosensors is based on the change of optical properties like absorbance, fluorescence or refractive index [6].

Another key topic of molecular nanotechnology is nanomachines, which control motion at the atomic scale [7, 8]. A nanomachine must, like any macroscopic machine, perform useful functions. It should contain a motor, where the energy supply (e.g. light, electric field, chemical environment, electric current) plays an important role. Such molecules can be synthesized completely, even though this is a difficult task for organic chemistry if the functionality and complexity is increasing, or assembled from various building blocks to supramolecular systems [9]. The major challenge in operating nanomachines is not only to achieve molecular motion, but also to control and read out the operation. An important issue in this regard is the information exchange with the macroscopic world, i.e. to control and prove the functionality of the nanomachines experimentally. It is not sufficient to detect that motion occurs, because for optimizing a nanomachine's operation a detailed understanding of the intramolecular processes is necessary. Finally, in order to approach useful nanomachines, the timescale of the operation and the possibility to repeat the operation in cycles are important properties.

Although the concepts of molecular machines are often similar to macroscopic machines, they cannot simply be considered as miniaturized versions, because matter behaves differently at the nanoscale. Gravitational forces and inertia can be neglected, due to small mass, and motion is dominated by physical/chemical interactions with molecules of the environment, for instance solution, or a supporting surface. On the other hand, thermal fluctuations (Brownian motion) are not important for macroscopic objects, but strongly prevail at the nanoscale [10].

Many approaches towards molecular nanomachines take advantage of concepts and processes that are known from nature. One example is DNA-based nanomachines, which are very suitable for the construction of three-dimensional objects by self-assembly, controlling their interaction through base sequences [11, 12]. By means of molecular motion, the protein family of myosins are very interesting, because their translational motion is similar to a 'walking' mechanism [13]. Much smaller molecules, based on an anthracene board, with in fact atomic scale dimensions, have been reported recently to move in a 'walking' mode, even 'carrying' CO_2 molecules [14, 15]. The rolling motion of carbon nanotubes on a graphite surface has been reported by directly imaging the different stages with an atomic force microscope (AFM) [16]. Furthermore, several molecular rotors [17] and surface-rolling molecules [18] have been proposed.

Figure 1.2 shows one of the most famous examples of a nanomachine, the rotaxane [9, 19, 20]. This molecule is considered as a molecular elevator, because the macrocyclic ring in its centre is mobile along the central molecular axis. Bulky groups that avoid disassembly of the supramolecular

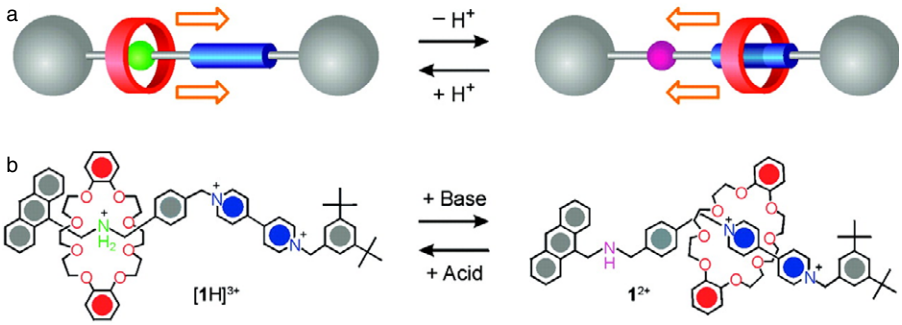

Figure 1.2. Principle of a 'molecular elevator'. (a) Schematic representation and (b) chemical structure of a bistable [2] rotaxane, containing two different recognition sites, to one of which the ring component is attracted much more than the other. The two different states of the molecule can be switched by an external stimulus, such as a change in pH. From [19]. Reprinted with permission from AAAS.

system terminate the axis. An important property of this molecular machine are the non-covalent interactions between the ring and the central board, allowing the motion of the macrocycle between different stable sites, where it is stabilized by hydrogen bonds or π–π stacking. By changing the chemical environment of the rotaxane between acid and base, the preferred position of the ring changes accordingly and it moves up and down, as shown in figure 1.2(b). It has been shown that this motion can also be induced by visible light [21], thus enabling different energy supplies of this 'motor'.

An important section of molecular nanotechnology is molecular electronics, the miniaturization of electronic devices to the atomic scale. As the top-down approach of the semiconductor industry, following Moore's law that transistor density doubles every three years [22], will reach its physical limits in the foreseeable future, devices of the size of single atoms or molecules will be required [23]. Hence, completely new strategies for the fabrication of nanocircuits at the molecular scale are necessary [24–28]. The ultimate goal is that single functionalized molecules are used as electronic devices connected by nanoscale wires.

Aviram and Ratner proposed as early as 1974 that a single molecule can act as a rectifier [29]. This concept, presented in figure 1.3, is based on the asymmetric conductance behaviour due to the donor–spacer–acceptor structure of the molecule. Similarly, the chemical structure of more complex molecules can be modified in order to design for example molecular wires or switches [24]. However, the first experimental studies of molecular devices were done more than 20 years later, when the conductivity through single molecules was investigated [30]. Molecular rectifiers, as proposed by Aviram and Ratner, were realized in a multilayer [31] or using single fullerene molecules [32] and the conductance was switched through conformational changes of the molecule [33]. An important class of molecules in this regard are carbon nanotubes with their characteristic physical properties [34]. Experiments have studied their conductivity [35], even over large distances of 1 μm [36], and their ability to be used in a transistor, by switching them from a conducting to an insulating state [37].

Additional to functionalized molecular devices, the wires and contacts represent the backbone of such a nanocircuit, as

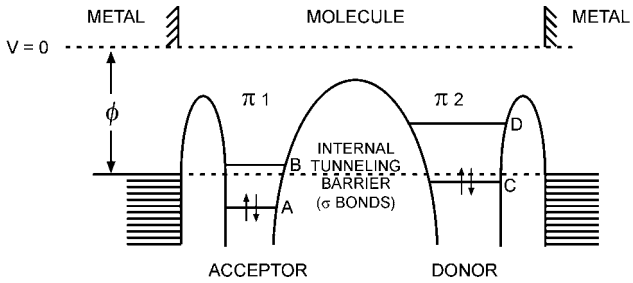

Figure 1.3. Energy versus distance of a single molecule rectifier device (schematic). B and D are the affinity levels and A and C the highest occupied levels, of acceptor and donor, respectively. By applying a bias voltage between the two metal electrodes, the molecular orbital levels shift with respect to the metal Fermi levels and to each other. Accordingly, the molecule exhibits different conductivities for the two bias polarities. Reprinted with permission from [29]. Copyright (1974) Elsevier.

they must enable efficient charge transport between the devices and electrodes. It is clear that the conductivity of molecular wires depends strongly on their chemical structure, as shown for a variety of possible molecular wires [38, 39]. On the other hand, the charge transport through contacts to other molecular devices or electrodes plays a fundamental role in the quality of a molecular device or any nanocircuit [40, 41]. It turned out that it is at least as important for the conductivity characteristics of a metal–molecule–metal system as the molecular core [42].

The preparation of nanocircuits from wires and functional building blocks is an important challenge, because molecules must be assembled efficiently in complex structures in an autonomous way [43]. While the ability of nanostructuring the supporting surfaces is important on the one hand [44], molecular recognition is a suitable tool to engineer the molecular structures [45, 46]. It has been shown that molecules are self-organizing through their interaction in various pre-defined topologies, even though mainly weak intermolecular bonds, with poor thermal stability, are explored [47, 48].

An important approach to determine the conductivity of a molecule between two electrodes is the so-called break junction, where a microfabricated electrode is broken at

its centre by mechanical deformation and the resistance of the metallic wire junction is measured [49]. In this way, the conductivity of very few molecules, which remain in the junction, can be determined directly, having the molecules strongly coupled by thiol groups to gold electrodes [50]. However, its application to single molecules is not straightforward because the conformation, environment and exact number of interconnected molecules remain difficult to determine [51].

The scanning tunnelling microscope (STM) is a powerful technique as it allows us to characterize and image precisely a single molecule (and its surrounding area) with sub-molecular resolution and to obtain information about its electronic and vibrational structure. Moreover, it can act as a tool to manipulate single molecules (and atoms) and thus to precisely probe their functions. Manipulation of molecules intends a controlled change in their position or conformation, a modification of their chemical or electronic structure or inducing chemical reactions. In order to suppress thermal motion of atoms and molecules and by means of experimental stability, the operation of the STM at low temperatures is advantageous. Experiments show that molecular displacement or conformational changes within a molecule can be mechanically induced by the STM tip [52–54]. Moreover, the tunnelling electrons can be used to induce several processes, for instance molecular rotation [55, 56] and vibration [57], by electronically/vibrationally exciting molecules [58]. Diffusion [59] or desorption [60] of molecules adsorbed on surfaces can be induced by the intense electric field present between the STM tip and the sample surface. Hence, the STM offers the possibility of creating a desired geometry by means of lateral displacement on a surface. It should be mentioned that manipulation of single atoms can also be done by atomic force microscopy (AFM) [61], which is of interest for non-conducting substrates.

This work presents experiments on functionalized molecules obtained with a (homebuilt [62]) low temperature STM (LT-STM) working at cryogenic temperatures around 5 K (the experimental set-up is described elsewhere [52]). The results focus on functionalized molecules, which represent model systems for several components in future applications of molecular nanotechnology and molecular electronics, adsorbed on metal surfaces. The substrate is acting on the one hand simply as a supporting surface and on the other hand as an electrode (while the other electrode is given by the STM tip).

2. Motion

The controlled manipulation of single molecules on surfaces with the tip of a scanning tunnelling microscope is of great interest for a detailed understanding of the molecular functions. Intramolecular conformations or molecular adsorption positions/geometries can be achieved on a surface which often would not be present after sample preparation, because they are energetically not favoured. At cryogenic temperatures (where molecular manipulation is usually done), instead, molecular configurations are 'frozen' due to the small thermal energy available. Furthermore, manipulation experiments not only give detailed insight into the molecular configurations and motions on a surface, but also represent a very interesting set-up for the study of interatomic forces (between STM tip and molecule) at atomic scale distances [63]. The various forces, active in such a junction, can in a first approximation be described by the Lennard-Jones potential (as a function of the interatomic distance between two noble gas atoms), consisting of attractive and repulsive interactions. The repulsive forces can, in contrast to the attractive ones, become very large at small interatomic separations. In the case of STM manipulation, chemical interactions and the role of the tunnelling current and the applied electric field must be taken into account. These forces can be studied during manipulation with high spatial precision if the relevant parameters (lateral and vertical tip position, applied bias voltage, tunnelling current) are systematically modified.

2.1. Lateral manipulation of molecules

The tip of a scanning tunnelling microscope is an important tool for the manipulation of single atoms [54, 64] and molecules [52, 65, 66], allowing their controlled displacement on a surface and even the construction of nanostructures or 'writing' at the atomic scale [67, 68]. Recently, it has even been shown how molecules can be used to trap single atoms while manipulated laterally on a metal surface [69]. Cryogenic temperatures, i.e. cooling of the sample, are advantageous for manipulation experiments, because in this way the thermal motion of atoms and molecules is frozen. The manipulation signal plays a fundamental role, because it gives direct insight into the molecular motion and thus the type of movement [64, 70]. This information cannot be obtained from the STM images before and after manipulation. Either the tip height signal (in the constant-current mode) or the tunnelling current (in the constant-height mode [71]) is recorded as a function of the lateral tip position. In the latter mode, the distance between the tip apex and a large molecule is not controlled by the STM feedback loop, i.e. by the electronic transparency of the molecule. Therefore, larger forces can be applied on the molecule compared to the constant-current mode [71].

The manipulation signal allows the characterization of the atomic or molecular motion due to different typical shapes [64]. The most important manipulation modes, pulling and pushing, are shown in figure 2.1. They both exhibit a saw-tooth shape with a periodicity d_o. As the adsorbate is hopping from one adsorption site on the surface to the next, the value of d_o corresponds directly to the interatomic distance of the substrate, if a symmetry direction of the surface is chosen. Accordingly, it deviates if the adsorbate hops not to the nearest site or not along a symmetry direction [72]. However, the slopes are different during pushing or pulling, having an ascending or descending edge, respectively. This can be understood from the mechanism during motion. In the first case ('pushing'; figure 2.1(a)) the tip is approaching the adsorbate laterally, which causes an increase of the current signal. As soon as the repulsive forces between tip and adsorbate are sufficient to overcome the diffusion barrier,

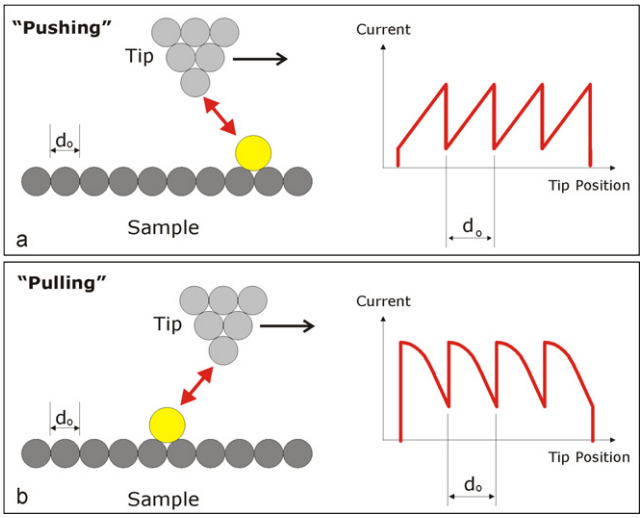

Figure 2.1. Principle of the lateral manipulation of an adsorbate on a surface by using the STM tip [64]. Either repulsive or attractive forces are driving the process, leading to a 'pushing' (a) or 'pulling' mode (b), respectively. The tip is moving in the schematics (left) according to the arrow. The manipulation signal (current curve at constant tip height), plotted to the right, reveals characteristic shapes and the periodicity d_o of the substrate.

the adsorbate hops to the next site. At the same time, the current signal drops abruptly and, subsequently, the next cycle starts with an ascending edge. The process is similar, but inverted, in the case of a pulling mode. Note that in any case the manipulation signal allows us to follow the atomic or molecular motion in real time. In addition to experiments, theory helps in the interpretation of the signals by simulating STM manipulation curves and can thus give precise details of the atomic or molecular motion [73–75].

The controlled manipulation of molecules on a surface is on the one hand of interest for the creation of nanostructures by the bottom-up assembly of matter at the atomic scale. On the other hand, it is the only way to bring single molecules into particular adsorption configurations which do not correspond to the energy minimum and are therefore not observed after deposition, and to obtain a detailed understanding of molecular 'nanomechanics' during such a motion. These capabilities are important for the development of molecular nanomachines [8].

2.2. *Rolling a molecular wheel*

Molecular machines, i.e. single molecules consisting of functional components, are a fascinating challenge in molecular nanotechnology [17]. The design of such a machine requires a detailed understanding of its mechanical motion [8]. Several studies in the last years have shown how molecules can be laterally displaced on a surface with high precision (see section 2.1). However, mainly *hopping* motions of molecules have been observed so far [52, 68, 76].

The best candidates for rolling motions are at first glance fullerenes, because they exhibit a spherical shape. Accordingly, the only clear example of a rolling molecule so far is a carbon nanotube, which is rolled on a graphite surface

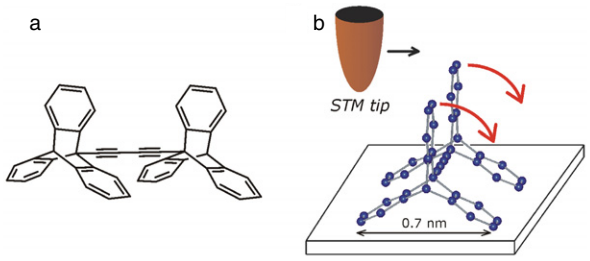

Figure 2.2. (a) Chemical structure of the wheel-dimer molecule ($C_{44}H_{24}$). (b) Scheme of a manipulation with the STM tip to induce a rolling motion (arrows indicate the tip movement and the rotation of the wheels, respectively). Reproduced with permission from [78]. Copyright (2007) Nature Publishing Group.

using an AFM tip [16]. However, the dimensions of this molecule exceed the atomic scale, having a tube circumference of 83 nm. On the other hand, the STM manipulation signal of a single C_{60} molecule on Si(100) was reported and presents a fine structure superimposed on the periodic manipulation 'hopping' signal, which was interpreted as a rotation of the fullerene during its hopping from one adsorption site to the next [77]. However, wheels are of greater interest by means of molecular machines, because their rolling motion should be directional. But so far, no *rolling* of a wheel has been demonstrated so at the nanoscale, even though this is a very useful motion at the macroscopic scale.

The rotation of single wheel molecules on metal surfaces has been induced thermally [79] or by STM manipulation [80], but in all cases the wheel was adsorbed flat on the surface, i.e. having its rotational axis perpendicular to the surface, and therefore unsuitable for the displacement of a molecular machine. A nanocar was synthesized by mounting four C_{60} molecules as wheels on a non-rigid molecular board [18], but no manipulation signal was reported to assess the possible rotation of these C_{60} wheels [81]. Wheel-shaped triptycene groups were mounted on a wheelbarrow molecule [82], but it was not possible to displace this molecule on the surface without modifying it.

Figure 2.2(a) presents the wheel-dimer molecule ($C_{44}H_{24}$), where two triptycene wheels are connected via a C≡C–C≡C axle. When adsorbed on a metal surface, this molecule exhibits two intramolecular degrees of freedom: the independent rotation of each wheel around the central axle. In order to induce a rolling motion by lateral STM manipulation (as schematically presented in figure 2.2(b)), a Cu(110) surface was chosen, which exhibits an anisotropic corrugation due to its close-packed rows of copper atoms in the $[\bar{1}10]$ direction. After deposition at room temperature, the molecules first saturate the step edges and then adsorb as isolated molecules on the Cu(110) terraces.

For a rolling motion, the orientation of the molecules with respect to the surface directions is of great importance. The wheel-dimer molecules adsorb in various orientations, in particular both with the molecular axle parallel and perpendicular to the copper rows. The STM image of a wheel-dimer is symmetric in these cases, with apparent wheel heights of 3.0 ± 0.2 Å. The most interesting configuration is the one

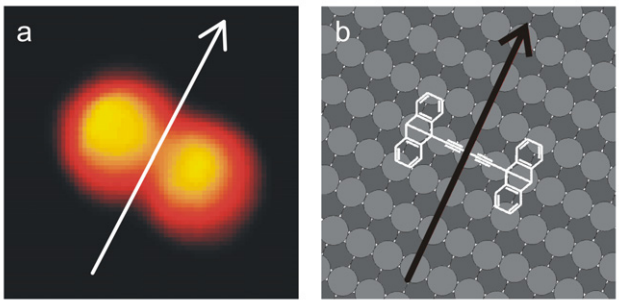

Figure 2.3. (a) STM image (3×3 nm^2) of a wheel-dimer molecule, oriented along the close-packed copper rows, before the manipulation and (b) the corresponding scheme (the arrows mark the pathway). Reproduced with permission from [78]. Copyright (2007) Nature Publishing Group.

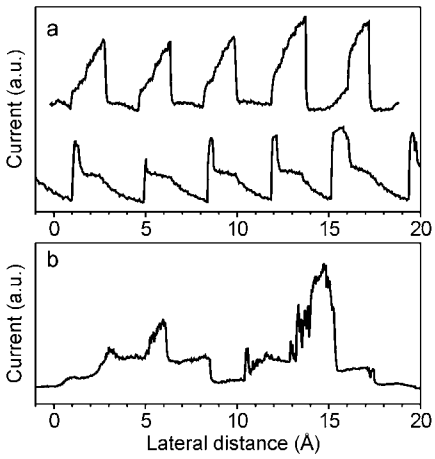

Figure 2.4. Tunnelling current signals during lateral manipulation: hopping (a) and rolling motion (b). While the periodicity of the signals in (a) corresponds to the atomic distances of the substrate, the rolling motion (b) exhibits a completely new, hat-shaped signal. Reproduced with permission from [78]. Copyright (2007) Nature Publishing Group.

having the molecular axle parallel to the copper rows of the substrate (figure 2.3), because the corrugation of the substrate becomes most efficient for a manipulation perpendicular to them. Calculations of the molecular conformation in this orientation show that the central molecular axle is located above a close-packed copper row and the lower benzene rings of the wheels are distorted as a result of their chemisorption on the Cu(110) surface [78]. The calculated STM image is in very good accordance with the experimental ones, consisting of two lobes at a distance of 8.7 ± 0.3 Å, which corresponds to the intramolecular distance between the two wheels of a single molecule.

Lateral motion of the molecules across the molecular axle (as indicated in figure 2.3) leads to typical periodic manipulation signals as presented in figure 2.4(a). These saw-tooth-shaped signals can be assigned to a pushing (ascending edge) and a pulling (descending edge) mode of manipulation [64]. The 3.6 Å periodicity of these signals corresponds to the distance between two atomic rows on the Cu(110) surface. Hence, the molecule is *hopping* from

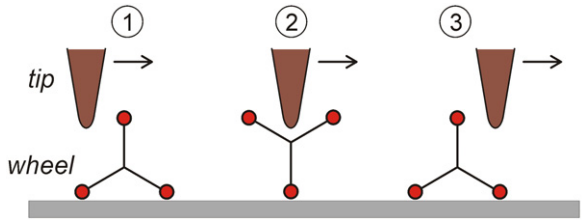

Figure 2.5. Scheme of the rolling mechanism: step (1) is the tip approach towards the molecule, the second step (2) is a 120° rotation of a wheel around its molecular axle and in the last step (3) the tip reaches the other side of the molecule. It shows that in principle only one rotation of a wheel can be induced (the direction of movement is marked by arrows). Reproduced with permission from [78]. Copyright (2007) Nature Publishing Group.

one adsorption site (i.e. copper row) to the next during the manipulation.

However, these are not the only observed signals. Also a completely different manipulation signal (figure 2.4(b)) has been recorded that is assigned to the *rolling* of a wheel within the molecule. Several arguments confirm this interpretation: first, the periodicity of the recorded signal is about 7 Å and therefore corresponds to a lateral motion of a wheel after a 120° rotation around the molecular axle (see figure 2.2(b)). Second, a standard hopping motion over two adsorption sites can be excluded because the signal does not show any pulling or pushing signature, which should be the case even during hopping over larger distances [72]. Instead, this hat-shaped signal exhibits one intense peak at the centre and smaller maxima on both sides. Even though the intensity distribution slightly changes from one case to another, the overall shape remains the same and has been recorded many times. An important difference between the two types of motions is that a rolling manipulation is always obtained at larger tip heights (vertical feed $\Delta z \leqslant 4$ Å; the initial tip height is about 7 Å) as compared to a hopping signal where the tip apex must be approached further down towards the surface ($\Delta z \geqslant 4$ Å). Hence, it is possible to choose in the experiment in a controlled way which kind of motion should be induced.

From the experimental results, the following mechanism is proposed in figure 2.5: the tip, at sufficiently large tip heights, induces a rolling motion of the molecular wheel, which undergoes a rotation of 120°. Notice that the hat-shaped signal is mirror symmetric, in contrast to the saw-tooth-shaped signal of a hopping mode. This observation is in accordance with the schematic model of the rolling mechanism [83], because the first and third steps are similar and therefore give rise to a comparable tunnelling current. The central step (2) reveals a more intense signal, due to the particular configuration of the molecule in this case, probably being oriented upright as proposed in figure 2.5.

The role of the surface corrugation becomes clear if manipulation experiments in various surface directions are compared. If the same lateral manipulation is performed on a molecule oriented perpendicular to the copper rows, the manipulation signal shows a clear pushing signature with a 2.5 Å periodicity, reflecting the close-packed structure along the rows. However, no rolling signal has ever been recorded for

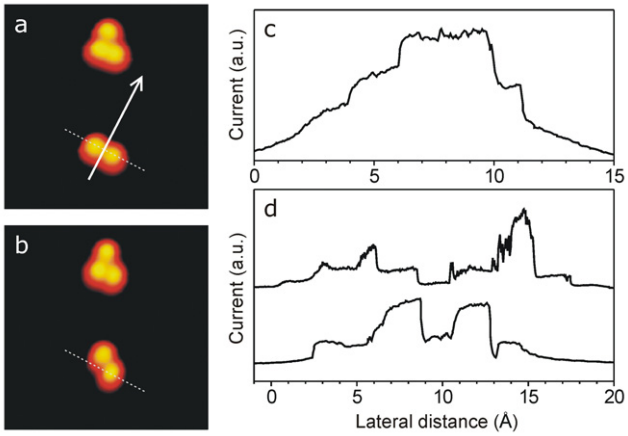

Figure 2.6. STM images (9×9 nm^2) before (a) and after (b) a rolling manipulation. The arrow marks the pathway of the tip apex during the manipulation and dashed lines indicate the initial position of the wheel-dimer molecule. Tunnelling current signals during a rolling manipulation are plotted in (c) and (d), revealing different numbers of hat-shaped signals. Reproduced with permission from [78]. Copyright (2007) Nature Publishing Group.

this set-up, because the anisotropic Cu(110) surface exhibits a much smaller corrugation in this direction [78]. A comparison with another surface orientation of the substrate, Cu(100), confirms this interpretation, as there very regular characteristic pulling and pushing signals were also recorded, but no evidence of a rolling signal has been found [78]. This is in agreement with the rather small corrugation of the Cu(100) surface, compared to Cu(110). Thus, due to the chemical structure of the wheel, a rolling motion occurs only if the molecule is manipulated perpendicular to its axle and along a surface direction of sufficient corrugation.

An important characteristic of the two kinds of motions arises from a comparison of the lateral displacements. When the molecule, oriented parallel to the copper rows (as in figure 2.3), is manipulated in a hopping or a rolling mode with equivalent tip apex pathways, the lateral displacement of the molecule turns out to be different (figure 2.6). In the pushing mode, the molecule follows the complete pathway of the tip (up to several nanometres, mainly limited by other molecules or step edges). In the rolling mode, instead, the molecule does not follow the tip apex up to the end, but one wheel moves and the other remains in its initial position (figure 2.6(b)). This difference is characteristic for the two types of motion: in the case of a hopping mechanism, the initial conditions for manipulation are restored after each hopping step, allowing large displacements. For a rolling motion (figure 2.5), the tip reaches the other side of the molecule after inducing a 120° rotation to a wheel. In this case, the starting conditions are not met any more and the displacement of the molecule is limited to a single rolling process.

The manipulation signal during the rolling motion (figure 2.6(c)) corresponds to a 120° rotation of the left wheel of the molecule. It is remarkable that in all cases where this signal has been observed one wheel is left in its initial position (and no long pathways occurred). The presence of two hat-shaped signals in figure 2.4(b) is rather an exception and can be explained by the alternate rotation of the two wheels. It turns out that the lateral distance, i.e. on the x-axis, between the two signals can vary, leading to a superimposition of the two hat-shapes in some cases. Figure 2.6(d) shows two examples, but also other distances between the two signals were observed. This effect is due to the variable starting point of the two wheel rotations, which depends on the precise tip apex shape.

These results show how the rolling of a molecular wheel can be induced in a controlled way with the STM tip. The only way to characterize unambiguously the kind of motion is the manipulation signal, which records the molecular movements and thus brings the information from the atomic to the macroscopic scale (the experimenter) in real time.

3. Molecular switches

In many possible future applications in the field of nanotechnology, electric circuits at the atomic scale should play an important role. This regards not only the miniaturization of integrated circuits ('molecular electronics'), but also the requirement that any information must be transferred between different components or to the macroscopic world. The optimal miniaturization would be reached if single molecules could be used [84]. An important component of any nanocircuit would be a molecular switch and intense research is being done on such molecules at the moment [33, 85–87]. A molecular switch undergoes a reversible transformation between at least two distinct stable switching states, usually geometrical or valence isomers, associated with different physicochemical properties based on a change in molecular geometry and/or electronic distribution [88]. The azobenzene molecule represents a very interesting example of such a molecular switch. Its operating mechanism is based on a reversible *trans–cis* isomerization of an N=N double bond. This process is conceptually related to the basic principle of vision in the human eye, where retinal molecules (bound to proteins) in the *cis* state undergo an isomerization process upon absorption of light. The corresponding conformational change is accompanied by a pulse that basically reflects the seeing process [89].

In the electronic ground state, azobenzene adopts two different conformations: a nearly planar *trans* and a non-planar, three-dimensional *cis* form [90]. The reversible switching between these two isomers is well investigated in solution and in the gas phase and occurs on both excited and ground state potential energy surfaces, whereby the ground state barrier for isomerization is typically overcome by photo-excitation [91–93]. Azobenzene has potential applications in a molecular device set-up as the conductance of the two isomers has been predicted to differ strongly [94]. The adsorption of azobenzene on metal surfaces has been studied by STM [95–97] and it has been shown that the molecule can be manipulated on Au(111) with the STM tip [98]. Moreover, very recent experiments have provided evidence that the isomerization of azobenzene [99] and of the azobenzene derivative Disperse Orange 3 [100] can be induced on Au(111) by STM.

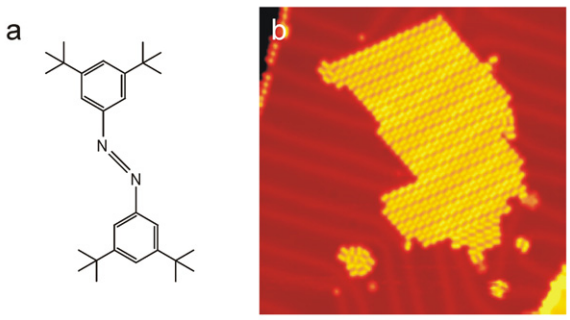

Figure 3.1. (a) Chemical structure of the TBA (3,3′,5,5′-tetra-*tert*-butyl-azobenzene) molecule. (b) STM image (40×40 nm^2) of a large area, showing single molecules, small disordered islands and a large, highly ordered molecular island. Reprinted with permission from [101]. Copyright (2006) American Chemical Society.

3.1. Growth of azobenzene derivatives on Au(111)

In the following, the switching of the azobenzene derivatives 3,3′,5,5′-tetra-*tert*-butyl-azobenzene (TBA), carrying four lateral *tert*-butyl groups (figure 3.1(a)), is studied. As recently shown, molecular spacers can be added to molecular wires or porphyrins in order to decouple the active part, i.e. the π-system, of the molecule from the metallic surface and therefore facilitate lateral manipulation with the STM tip [52]. In the present case, there are two distinct advantages of this particular substitution pattern: first, it increases the separation between surface and the azobenzene π-,system thereby leading to increased surface mobility and potentially lower electronic coupling. Second, its set of four symmetrically placed labels facilitates conformational analysis. Furthermore, it is important that the spacers do not significantly alter the electronics of the azobenzene chromophore and do not impart steric hindrance to the isomerization process.

Figure 3.1(b) shows an overview STM image of TBA molecules on Au(111). The molecules are mobile after adsorption, as they cover step edges and form islands, but are also found isolated on terraces. Islands formed by fewer than about 40 molecules are disordered, i.e. the molecules are not equally oriented. As the number of molecules increases, the intermolecular interaction leads to the formation of ordered islands. Each molecule appears as four lobes with an apparent height of 2.7 ± 0.1 Å arranged in a rhombic shape (figure 3.2(a)).

According to the dimensions of the molecule in the gas phase, the lobes can be assigned to the *tert*-butyl groups while the central azobenzene part is not visible. All observed molecules are in the same planar configuration, corresponding to the *trans* isomer, which is known to be the energetically favoured configuration in the gas phase [90]. The complete absence of *cis* isomers on the surface is expected, because any heating process (for deposition) increases the fraction of the *trans* isomers at the expense of the *cis* molecules. The position and orientation of individual molecules inside the islands is shown in figure 3.2(b): the molecules form parallel rows indenting with each other.

3.2. Isomerization

The isomerization capability of TBA molecules has been studied in solution by using absorption spectroscopy (figure 3.3). The $\pi \rightarrow \pi^*$ electronic excitation around 325 nm wavelength is a characteristic measure for the number of *trans* isomers present [102]. The decrease of this absorption band in (a) upon illumination can thus be assigned to the *trans* $\rightarrow$ *cis* isomerization. On the other hand, the *trans* isomers are restored (*cis* $\rightarrow$ *trans* isomerization) if the solution is kept at an elevated temperature (without illumination) for some time (figure 3.3(b)). Hence, both the photochemical and the thermal isomerization behaviour typical for azobenzene derivatives are successfully induced, which shows that the *tert*-butyl legs attached to the azobenzene core do not hinder isomerization of the molecules.

The isomerization process has been studied in ordered molecular islands, where a large number of molecules is available. In figure 3.4 an example of a switching experiment is shown. To induce the isomerization, subsequent voltage pulses have been applied with the STM tip always at the same position

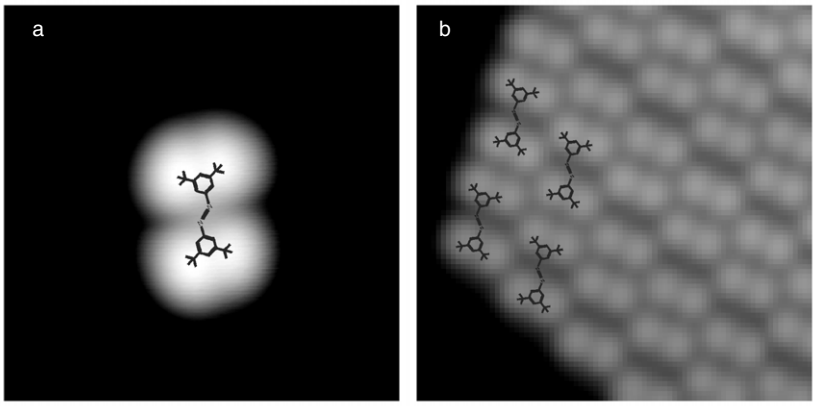

Figure 3.2. (a) STM image (4.6×4.6 nm^2) of a single TBA molecule, appearing as four lobes, with the superimposed chemical structure. The exact adsorption configuration within an island is determined in (b) from the corner of an island (the choice of the molecular chirality for the superimposed molecular model in (b) is arbitrary). Reprinted with permission from [101]. Copyright (2006) American Chemical Society.

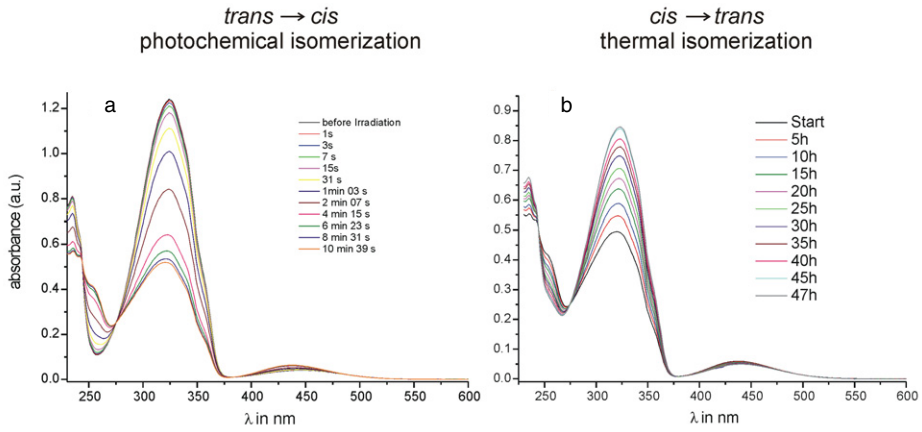

Figure 3.3. Isomerization of TBA molecules in solution (cyclohexane). (a) Photochemical *trans* → *cis* isomerization at 25 °C using a 1000 W XBO light source equipped with interference filter $\lambda_{maxT} = 313$ nm (11% T, FWHM = 10 nm). (b) Thermal *cis* → *trans* isomerization at 50 °C solution temperature. Experiments done by Maike Peters. Reprinted with permission from [101]. Copyright (2006) American Chemical Society.

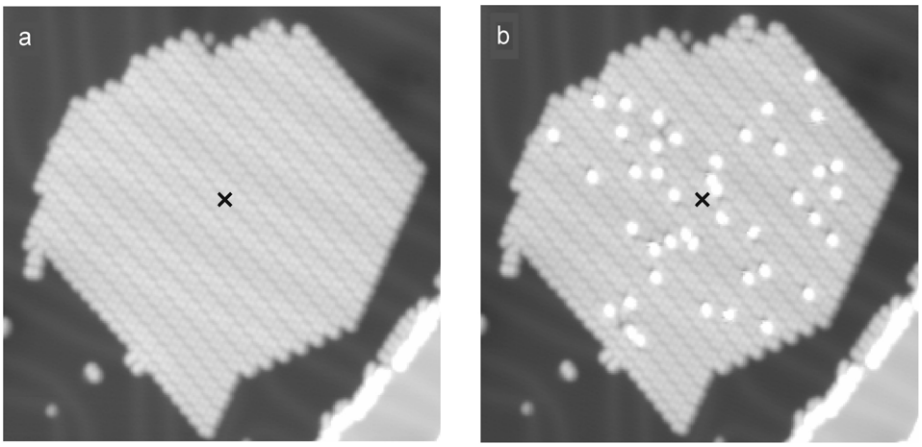

Figure 3.4. (a) Island of TBA molecules containing about 400 molecules, all in the *trans* state (370 × 370 Å^2). Subsequent voltage pulses (20 s, $V_m = 2$ V, tip height = 6 Å) are applied at the position indicated by the cross. (b) STM image of the same island after nine pulses: 43 molecules have been switched to the *cis* form. Reprinted with permission from [101]. Copyright (2006) American Chemical Society.

above the island. After each pulse an STM image is recorded. The image after nine equivalent pulses is shown in figure 3.4(b) (the complete series of 48 pulses is available as a movie [101]). As one can see, many molecules have changed appearance, showing a larger height of 4.1 ± 0.3 Å. The bright molecules are stable, and to let them return to their initial appearance a further pulse must be applied, as shown in figure 3.5. Such switching experiments can be reproduced several hundred times, allowing the conclusion that the observed changes are due to the isomerization of single molecules from the *trans* to the *cis* form, and back to the *trans* form. The reversibility of the experiment and its high reproducibility exclude molecular dissociation or the presence of any contamination as the cause for the observed change of the molecular appearance. The switching of an isolated molecule is very rare, because, under the effect of a voltage pulse, the molecule can move or rotate, thereby efficiently competing with the isomerization process. This effect is avoided in the islands, when the molecules are stabilized by each other.

Figure 3.5(a) shows a *cis* isomer in a molecular island in detail, imaged after a switching pulse. As one can see, the isomerization process has no consequence for the neighbouring *trans* molecules, which remain unchanged. The *cis* form appears with a bright central intensity maximum, while three lateral lobes in an approximately triangular shape can be resolved, completely different from the planar *trans* conformation.

Based on the STM images, the model in figure 3.5(c) is proposed for the *cis* conformation: one of the two phenyl rings is standing upright with a *tert*-butyl leg pointing upwards, giving rise to the intense lobe in the STM images. The second leg of this phenyl ring is located close to the surface, causing the weak intensity maximum above the central lobe in figure 3.5(a). The other phenyl ring is almost unchanged compared to the *trans* state and therefore shows a similar appearance of two lobes (at the bottom of the STM image in (a)). Hence, it turns out that the *cis* isomer is not planar, in agreement with the molecular conformation in the gas

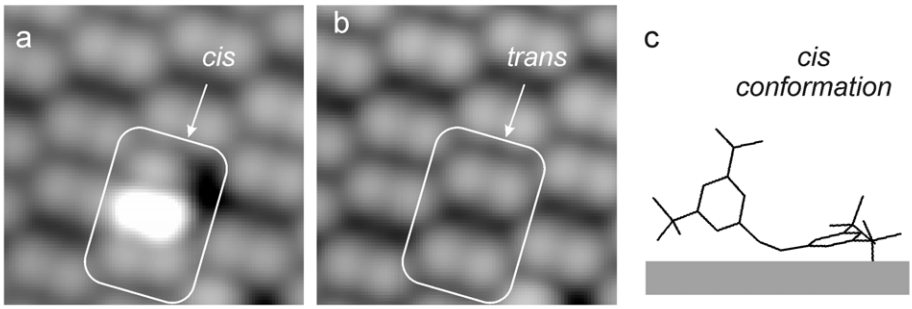

Figure 3.5. (a) and (b) STM images (3.5×3.5 nm^2) of a few molecules within an island before and after applying a voltage pulse, causing the switching of the *cis* isomer in the centre to the *trans* state (marked by a rectangle). (c) shows the proposed conformation of the *cis* isomer (see text). Reprinted with permission from [101]. Copyright (2006) American Chemical Society.

phase [90] and as observed by STM [99] for azobenzene molecules on Au(111).

Furthermore, switching of the molecules is accompanied by a shift of the LUMO orbital [101], strongly pointing towards an isomerization process (*trans* and *cis* isomers exhibit different electronic structures and band gaps [103]). The particular appearance of the *cis* isomers was precisely confirmed very recently by STM experiments, where the same molecules are isomerized by light, similar to photo-isomerization in solution, but being adsorbed on a Au(111) surface [97].

In order to understand the driving mechanism of the induced isomerization, the threshold voltage necessary for switching the molecules has been determined, for the *trans* → *cis* and for the *cis* → *trans* process, as a function of the tip height above the sample (figure 3.6). As one can see, the threshold voltage for the isomerization, possible with positive and negative voltage polarities, increases with the tip height in all cases. While this shift is rather small at low tip heights, where the process is likely driven by the tunnelling electrons (a mechanism that has been suggested for isomerization of azobenzene derivatives [99, 100, 104]), it can become very pronounced at larger tip heights, where the tunnelling current (decreasing exponentially with the distance) is much smaller. Data fitting shows an approximately linear relationship between the threshold voltage and the tip height with slopes between 0.1 and 0.7 V Å^{-1}.

This linear dependence strongly points to an electric-field-induced isomerization. In this case, the electric field in the STM junction deforms the potential landscape of the molecule along its reaction path in the ground state, allowing the switching process. This interpretation is in agreement with the observation that isomerization can be obtained even at large tip heights in figure 3.6, where the tunnelling current goes to zero (up to 36 Å have been measured), as electric-field-driven processes should not depend on the tunnelling electrons. Note that the observed steep slopes cannot be explained by isomerization processes induced by molecular excitation through field emission. The electric field mechanism has not been observed experimentally so far, but was recently explained by theoretical calculations [106, 107]. The different slopes for positive and negative voltages in the case of *trans* → *cis* isomerization with respect to the *cis* → *trans* case are likely due to the delicate balance between the intrinsic dipole moment of the molecule and its polarizability for the different adsorption geometries and reaction paths.

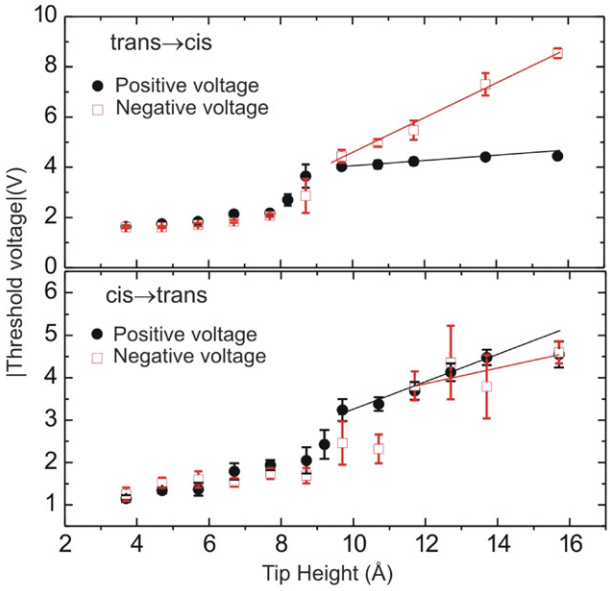

Figure 3.6. Plot of the threshold voltage as a function of tip height for the *trans* → *cis* isomerization (top) and for the *cis* → *trans* isomerization (bottom) for positive (electric field points towards the STM tip) and negative voltage polarities. The experimental points have been measured by fixing the tip height and applying a voltage pulse for a fixed time. This voltage was increased until at least one switched molecule in a lateral area of 80 Å × 80 Å from the tip position was observed. The tip height refers to the gold surface (calibrated by recording $I(z)$ curves [105]). The linear fit of the data is done for points above 9.5 and 11 Å (*cis* → *trans* at negative voltages). Reprinted with permission from [101]. Copyright (2006) American Chemical Society.

The isomerization behaviour of the same system, TBA molecules on Au(111), has recently been studied by two-photon photoemission (2PPE) spectroscopy [108], a method that integrates over the surface, in contrast to STM (figure 3.7). Two important changes can be seen in the spectra after illumination (figure 3.7(a)): An intensity loss of the $n = 1$

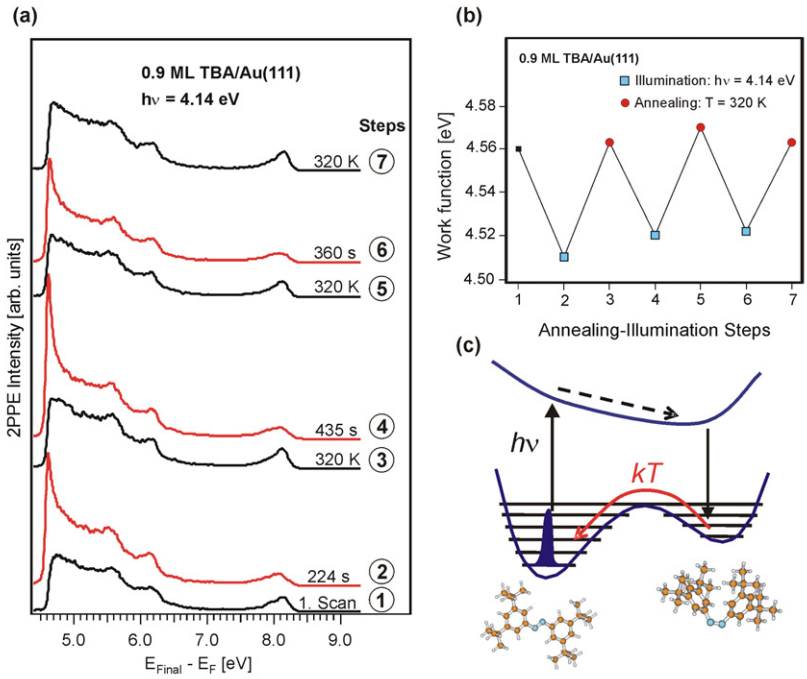

Figure 3.7. (a) 2PPE spectra taken at a photon energy of 4.14 eV of 0.9 ML TBA/Au(111) before (step 1) and after illumination for 224 s (step 2), and cycles of illumination and annealing steps. (b) Dependence of the work function of the TBA-covered Au(111) on UV-light exposure and annealing. (c) Scheme of the reversible isomerization (the left minimum corresponds to the *trans* and the right to the *cis* state). Reproduced with permission from [108]. Copyright (2007) Elsevier.

image potential state (at around 8.1 eV) and an increase of the photoemission intensity near the secondary edge (4.7 eV). These effects are assigned to the successful *trans* → *cis* isomerization of the molecules, whereas the latter one might be caused by an unoccupied final state of the *cis* isomers as the electron kinetic energy of this peak does not change with the photon energy [109]. Furthermore, the isomerization is accompanied by a decrease in the work function of about 50 meV. This effect can be explained by the appearance of rather large dipole moments characteristic for the *cis* isomer (whereas the *trans* molecules have a vanishing dipole moment in the planar configuration) [106]. After the photo-induced switching, the *cis* TBA molecules were thermally relaxed to the *trans* state by annealing of the sample at 320 K. Accordingly, the initial appearance of the photoemission spectrum in figure 3.7(a) can be restored several times. This behaviour clearly demonstrates the reversibility of the isomerization process, which becomes even more evident from the development of the work function (b). A scheme of the entire reversible isomerization cycle induced by UV light (*trans* → *cis*) and heat (*cis* → *trans*) is shown in figure 3.7(c).

4. Covalent intermolecular connections

A key goal of nanotechnology is the development of electronic devices at the atomic scale. The ultimate miniaturization would be reached if single molecular building blocks, which inherit certain functions (e.g. switching or rectifying), could be connected on a supporting surface, leading to the so-called molecular electronics [24]. The main challenge in this regard is the controlled assembly of molecules into desired architectures. The ability of molecules to form supramolecular structures on surfaces by self-assembly has attracted considerable attention in the last years [47, 48, 110–112]. The derived patterns, with dimensions almost up to the millimetre range [113], are held together by different non-covalent intermolecular forces such as hydrogen bonding [48, 111, 114, 115], π–π stacking [113], dipolar [116], van der Waals [117] or metal–ligand [118] interactions. However, strong, i.e. covalent, intermolecular connections are required in possible applications for two reasons [26]: these bonds would be highly stable [119] and could facilitate efficient charge transport [40] in contrast to supramolecular structures. Note that such large networks are difficult to manufacture by traditional repetitive chemical synthesis and are hard to deposit onto surfaces [120].

It has been shown in the last years that the scanning tunnelling microscope (STM) can be used as a tool to perform single-molecule chemistry [58]. Figure 4.1 shows an example of how bonds between single atoms and molecules can be broken and built, thus inducing a complete chemical reaction at the single molecule level [121]. In a first step, iodobenzene molecules are dissociated into an iodine atom and a benzene ring (figures 4.1(a) and (b)). The different components are identified by their characteristic appearance. Then, after lateral manipulation of the molecules, a chemical bond is formed between two benzene rings, producing a biphenyl molecule (c), whereas the reaction is driven by the tunnelling electrons in the junction (similar to the creation of carbon dioxide from CO and an oxygen atom [122]). The successful reaction leads to a

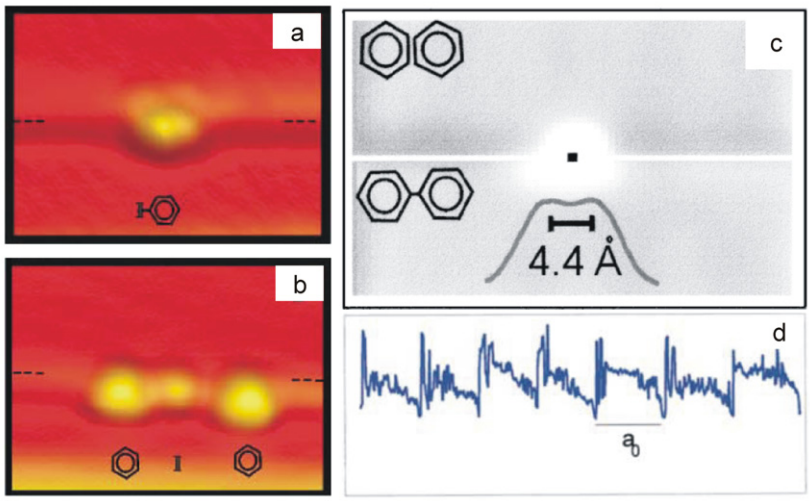

Figure 4.1. (a) STM image (60 Å × 42 Å) of a iodobenzene molecule adsorbed at a step edge on Cu(111). (b) The STM image after the dissociation shows two phenyls (triangular shape) and an iodine atom (centre) adsorbed at a (100)-type step edge after tip-induced dissociation of two iodobenzene molecules. The other iodine was transferred to the tip apex. (c) Background-subtracted STM image (24 Å × 14 Å) with a phenyl couple in its centre. The upper and lower parts correspond to the stages before and after the chemical association. The tip height profile across the centres of the synthesized biphenyl molecule is indicated. (d) Tip height curve during lateral movement of the created biphenyl molecule, revealing a characteristic pulling behaviour of the entire molecule. Reprinted with permission from [121]. Copyright (2000) by the American Physical Society.

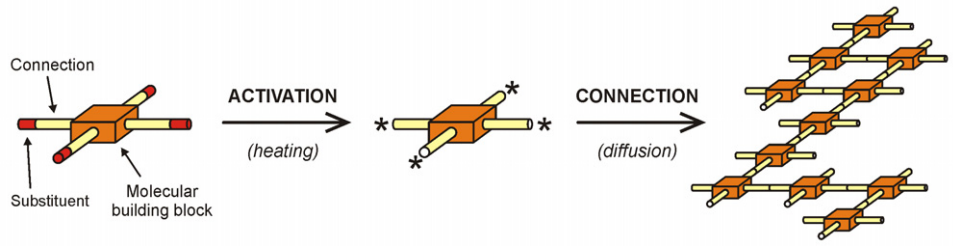

Figure 4.2. Concept of the formation of covalently bound networks by activation and connection of molecular building blocks. Reproduced with permission from [123]. Copyright (2007) Nature Publishing Group.

changed appearance of the molecule, revealing a double lobe height profile instead of a single maximum before the reaction. The experimental proof for the formation of a covalent bond is made by lateral manipulation with the STM tip. Upon pulling at one end of the biphenyl molecule, the entire molecule follows the pathway of the tip (figure 4.1(d)), a behaviour that is unlikely for weak intermolecular bonds. However, even though such experiments open exciting possibilities for single-molecule chemistry with the STM, it is not suitable for applications where a large number of molecular building blocks need to be connected in a desired architecture.

4.1. Bond formation by activation of molecular side groups

In the following, a method is presented that overcomes the limitation of STM induced reactions and allows the creation of covalently bound nanoarchitectures, i.e. macromolecular structures with controlled shape and size, from a large number of molecules.

The concept is illustrated in figure 4.2: a chemically stable, central molecular unit is equipped with several, symmetrically placed legs. After dissociation of substituent atoms in the first step by heating (activation), the monomer building blocks are connected with each other through the activated legs directly on the surface upon thermal diffusion. The ability of organic chemistry to design and synthesize molecules with a different number and relative arrangement of pre-defined connection points allows the construction of various topologies. The central conditions for this procedure are the maintenance of the chemical structure of the molecular building block during activation, sufficient mobility of the molecules after deposition and the availability of reactive side groups even on the supporting surface (chemical reactions with the substrate or contaminants must be avoided).

It is important that the reactive legs can be activated selectively, i.e. without breaking the other bonds. For this purpose, carbon–halogen bonds, exhibiting much smaller binding energies as compared to the central framework [121, 124], were chosen, while a porphyrin with four phenyl legs constitutes the central building block. This molecule is chemically stable and, moreover, mobile on metal surfaces [116, 125], which is essential for efficient intermolecular connection.

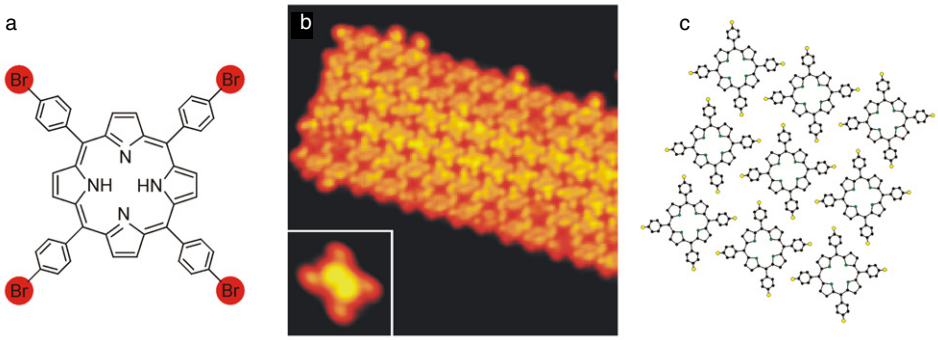

Figure 4.3. (a) Chemical structure of the Br_4TPP molecule (substituent Br atoms are marked by circles). (b) STM image (20×20 nm^2) of a molecular island on Au(111) after deposition at low evaporator temperatures of 550 K (the inset shows a single TBrPP molecule; image size: 4×4 nm^2) with the corresponding scheme in (c). Reproduced with permission from [123]. Copyright (2007) Nature Publishing Group.

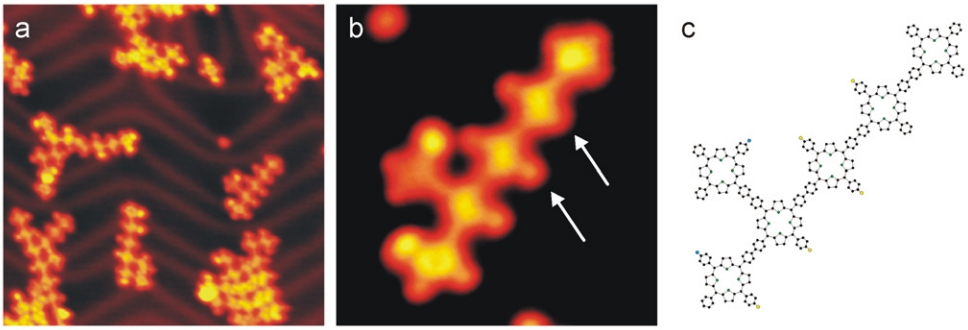

Figure 4.4. (a) STM image (41×41 nm^2) for deposition at an elevated evaporator temperature of 610 K, causing the formation of networks. (b) STM image (9×9 nm^2) of a nanostructure of six molecular building blocks. The arrows indicate molecular legs with (lower arrow) and without (upper arrow) Br atoms. This network is drawn schematically in (c). Reproduced with permission from [123]. Copyright (2007) Nature Publishing Group.

At each leg bromine was used as the labile substituent atom to be dissociated in a controlled manner, leading to the tetra(4-bromophenyl)porphyrin (Br_4TPP) molecule (figure 4.3(a)). After deposition of the molecules onto clean Au(111) from an evaporator at 550 K temperature or below, large islands were found as a result of molecular diffusion on the surface (figure 4.3(b)). A detailed analysis of these islands shows that they consist of intact Br_4TPP molecules in a close-packed structure, minimizing the intermolecular distances (c). The molecules in the outermost rows of an island appear typically different from the inner part, because they often have only three (of four) Br atoms attached. This observation suggests the dissociation of bromine atoms from a small fraction of the molecules at the used Knudsen cell temperature. However, the major part (more than 90%) of the molecules remains intact with all four Br atoms present. The exact number of bromine atoms, attached to the tetra(phenyl)porphyrin (TPP) molecule, was determined by a controlled dissociation of one Br atom after the other from the molecular core with voltage pulses between tip and surface of about 2.2 V [123]. Thus, a higher bias is required than for iodine phenyl separation [124], in accordance with the larger bond dissociation energy of the C–Br bond as compared to a C–I bond.

The behaviour of the molecules changes fundamentally if the evaporator temperature is raised to at least 590 K. Most of the molecules become 'activated', with the loss of several Br atoms. Upon thermal diffusion, these activated molecules react with each other to form intermolecular chemical bonds, thereby building macromolecular nanostructures of various shapes on the surface (figure 4.4).

Chains are the preferred shape, as the formation of two-dimensional networks requires more than two connection points between the molecular building blocks. Note that some of the molecular building blocks have all legs activated, while others still have inactive legs with Br atoms attached (marked by arrows in figure 4.4(b)). Each molecule provides up to four possible connections to other molecules, resulting in two-dimensional patterns of a different number N of bound molecules.

Various examples of such networks— trimer, tetramer, pentamer and octamer— are shown in figure 4.5. Due to the reduced mobility and diffusion of connected building blocks, the growth is self-limited and the number of networks on the surface decreases with increasing N. Note that the formation of the networks is not a self-assembly process, because it is not reversible [110].

4.2. Nanoarchitecture

In order to show the ability of controlling the nanoarchitecture of the macromolecular structures, different TPP-based

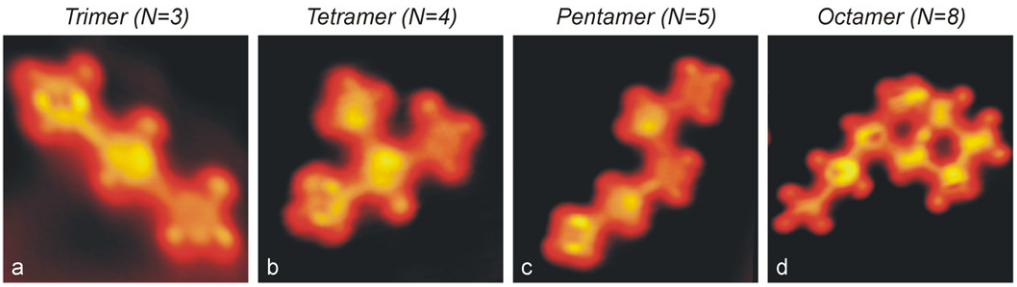

Figure 4.5. TPP nanostructures with various numbers N of involved molecular building blocks. Reproduced with permission from [123]. Copyright (2007) Nature Publishing Group.

molecules with one, two or four Br substituents have been synthesized (figure 4.6). All molecules are found intact on the surface (in clusters and ordered islands) if low evaporator temperatures are used, and their different structures are reflected in the respective STM intensity distribution (figure 4.6). In the case of sufficient heating, the molecules become activated and connect on the surface. Characteristic molecular arrays are found on the surface, whereas the topology precisely corresponds to the molecular design (figure 4.6): if only one Br substituent is used (BrTPP), exclusively dimers and no larger macromolecular structures are observed, because each building block provides only one reactive site.

On the other hand, the design of porphyrin building blocks with two Br atoms in a linear geometry (*trans*-Br_2TPP) leads to the formation of long, linear chains. Accordingly to the modification of the molecular building blocks (as compared to BrTPP), their growth is not limited to dimers. Note that abrupt curvatures (marked by an arrow in figure 4.6(h)) are caused by the attachment of two chains upon weak interaction. They can be separated by lateral manipulation. Finally, the use of four Br substituents at all phenyl legs (Br_4TPP; figure 4.6(c)) enables the construction of two-dimensional networks (as described above).

In agreement with these observations, no macromolecular structures can be formed if TPP molecules without Br substituents are used (figure 4.7). Instead of forming covalent bonds, the molecules are weakly bound in islands or clusters, which can easily be separated upon lateral manipulation. Starting with three weakly bound TPP molecules in (b), manipulation leads to their separation in (c) and (d). Note that the tip pathway always starts at the terminal molecule of the chain, thus pulls the molecules. Such a separation cannot be done if covalent intermolecular connections are present.

The intermolecular bonds turn out to be relatively strong compared to bonds within the molecular islands, causing the entire molecular nanostructures (dimers, chains and networks) to follow the pathway of the tip without fragmentation (figure 4.8). It is important to note that manipulation experiments are done by starting the tip pathway at the terminal molecular building block of a network (arrow in figure 4.8), thus 'pulling' on one end with the STM tip. The motion of the macromolecule can be clearly seen with respect to the herringbone reconstruction of the Au(111) substrate. This is a convincing experimental proof (similar to figure 4.1) of a strong intermolecular bond, because such a large molecular assembly would not follow the first (pulled) molecule in the case of weak connections. Furthermore, the experimentally determined distance between two neighbouring porphyrin cores in a nanostructure (17.2 ± 0.3 Å) is in agreement with the calculated distance (17.1 Å) and hence consistent with the formation of a covalent bond. This observation is in contrast to the case of *para*-diiodobenzene molecules, where the phenyl rings—after dissociation of the iodine atoms upon adsorption on the Cu(111) surface—do not form covalent bonds between them [126].

These arguments confirm the interpretation of covalent bonds between the building blocks. Note that hydrogen bonds, π–π stacking, and metal–ligand interaction can be excluded due to the chemical structure and adsorption geometry of the molecules. As a consequence, covalently bound nanostructures should in principle be capable of charge transport between the molecular building blocks, as it is known that porphyrin oligomers can exhibit electronic conjugation [127].

The covalent nature of the intermolecular bonds is also proven by spectroscopy measurements (figure 4.9) and density functional theory (DFT) calculations (figure 4.10). The appearance of the nanostructures in the STM images changes fundamentally upon an increase of the bias voltage. While at low voltages the dimer in figure 4.9(a) appears with homogeneous contrast, an intense protrusion is visible at the connection between the two porphyrin molecules when the voltage is raised to 3 V. Scanning tunnelling spectroscopy data (figure 4.9(c)) show that this protrusion is associated with a broad peak around 3 eV centred around the intermolecular connection, which is absent on the bare leg. These observations suggest the presence of localized orbitals at the connection as supported by DFT calculations of an isolated, covalently bound dimer of porphyrin molecules (figure 4.10).

The calculations [123] show that the covalent bond is formed between the two neighbouring phenyl legs, with corresponding C–C bonding (σ) and anti-bonding (σ^*) orbitals. The C–C bonding results in a strong interaction between the two unoccupied, anti-bonding π orbitals on these two legs, forming in-phase and out-of-phase combinations split by 1.3 eV. The in-phase combination gives rise to an enhanced orbital density on the connection away from the porphyrin (figures 4.10(a) and (b)) around 2.8 eV above the highest occupied molecular orbital (HOMO) level. This energy can be compared with experiments because calculations of

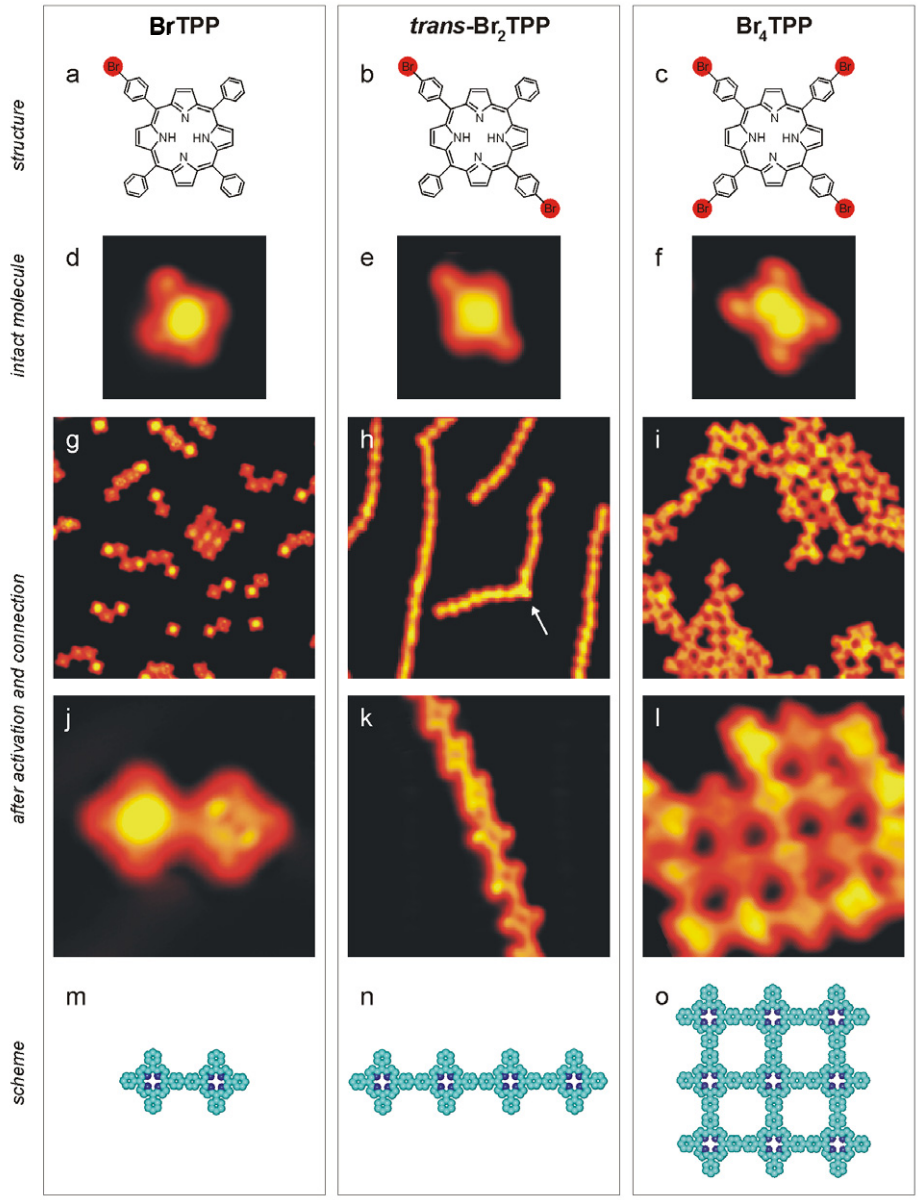

Figure 4.6. Different monomer building blocks with one (left panel), two (middle) and four (right) Br substituents. (a)–(c) Chemical structures and (d)–(f) corresponding STM images of single intact molecules (all 3.5 × 3.5 nm^2), where the brominated legs appear larger. (g)–(i) Overview STM images (all 30 × 30 nm^2) and (j)–(l) details of STM images of the formed nanostructures ((j) 5 × 5 nm^2, (k) 10 × 10 nm^2 and (l) 8.5 × 8.5 nm^2). The corresponding chemical structures are shown schematically in (m)–(o). Reproduced with permission from [123]. Copyright (2007) Nature Publishing Group.

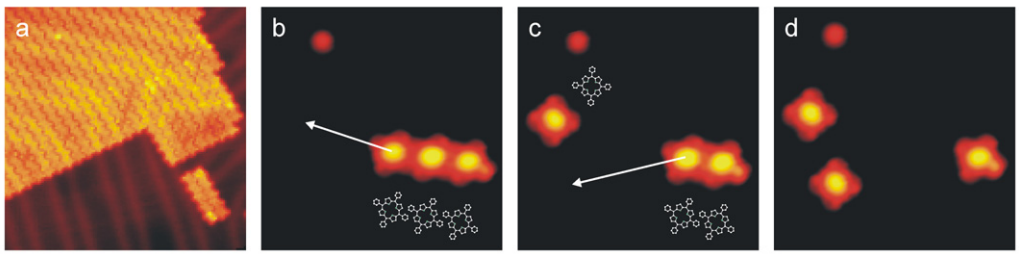

Figure 4.7. (a) STM image (30 × 30 nm^2) of a molecular island of TPP molecules. (b)–(d) Series of STM images (9 × 9 nm^2) during the manipulation of a cluster (the molecular configuration is indicated schematically while the arrows mark the pathway of the STM tip). Reproduced with permission from [123]. Copyright (2007) Nature Publishing Group.

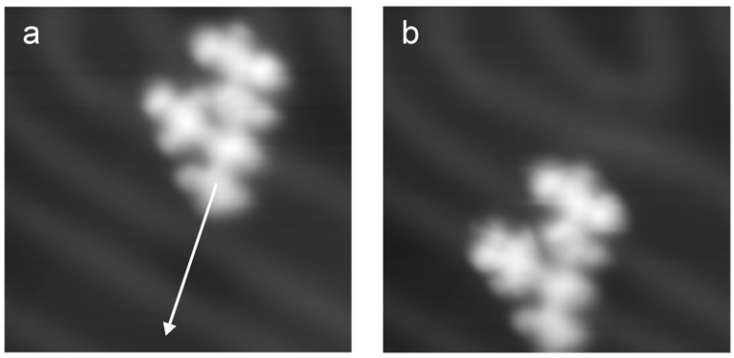

Figure 4.8. STM images (15×15 nm^2) before (a) and after (b) the lateral manipulation of a molecular pentamer (network with $N = 5$) using the STM tip (the arrow indicates the tip pathway). Note that the pentamer is pulled at the terminal molecule. Reproduced with permission from [123]. Copyright (2007) Nature Publishing Group.

a TPP molecule adsorbed on a Au(111) surface show that the molecule is weakly adsorbed and that the HOMO level is nearly aligned with the Fermi level. The protrusion seen in the STM images and the peak in the spectroscopy data at biases of around 3 V can be rationalized by the increased local density of states above the connection (figure 4.10(c)) due to this particular electronic state.

Finally, it should be mentioned that the activation of the molecules can achieved by two methods, either choosing a sufficient evaporator temperature or by heating of the sample at 590 K after deposition of intact molecules (i.e. avoiding Br dissociation during deposition). The second method is of great interest for the selective activation of different molecular sites, in principle leading to complex network architectures. It should be emphasized that the availability of these two complementary techniques can be of great advantage, e.g. if the molecular weight does not allow activation and evaporation at the same time or—on the other hand—if sample heating must be avoided due to previous preparation of films or nanostructures on the surface.

5. Outlook

The reported experiments give a detailed insight into the behaviour of functionalized molecules. The next steps in this research field should use these findings on the motion and operation of such molecules to improve the functional efficiencies. In view of the potential of such model systems for future applications, following experiments should concentrate on more complex systems, considering the obtained results for the improvement of the molecular functions.

After proving the rolling of a molecular wheel at the atomic scale, a logical consequence is to study first of all other types of molecular wheels. It is important to understand how the chemical structure changes the rolling motion and the diffusion barrier, which must be overcome. Moreover, the exact role of the surface corrugation, required for a rolling motion due to the presented results, needs to be understood. In other words: what corrugation is necessary to enable a rolling motion and, on the other hand, what is the limit of the surface corrugation? In analogy to the macroscopic world, it would be interesting to study whether it is possible to overcome

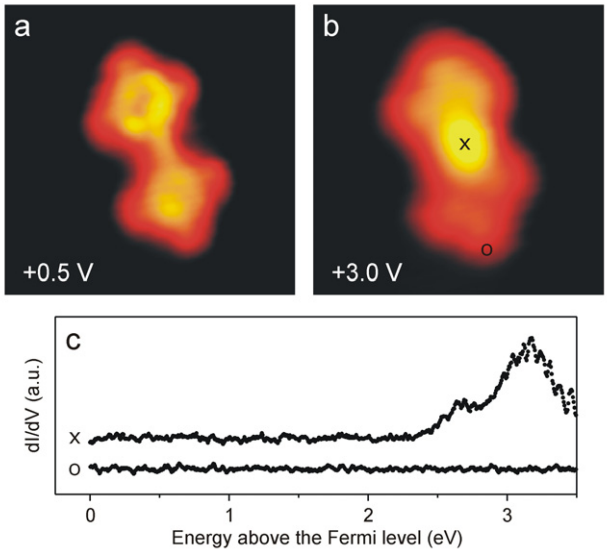

Figure 5.9. STM images (5×5 nm^2) of a porphyrin dimer at different sample bias voltages of 0.5 V (a) and 3.0 V (b) reveal a difference in the electronic structure. (c) Experimental $\mathrm{d}I/\mathrm{d}V$ curves. The upper curves are obtained at the connection ($\times$) between two molecular units while the lower curves are obtained above a bare leg (O) (the two positions are indicated in (b)). From [123], with permission.

obstacles (e.g. step edges or nanostructures) on a surface by a rolling motion, which cannot be done by a hopping motion of a molecule. In this way, new diffusion properties of molecular machines would become possible. In a next step, it would be of great interest to incorporate a suitable type of wheel into a larger molecule, creating a real nanovehicle based on a rolling motion. The directionality of the lateral movement on the surface, caused by the rolling motion of the wheels, should be controlled by an appropriate design of the nanomachine. The use of nanostructured surfaces could be of interest in this context.

The next steps in the research field of molecular switches are twofold. On the one hand, it is important to precisely study the dependence of the switching mechanism on the chemical structure of the molecule, focusing on the switching

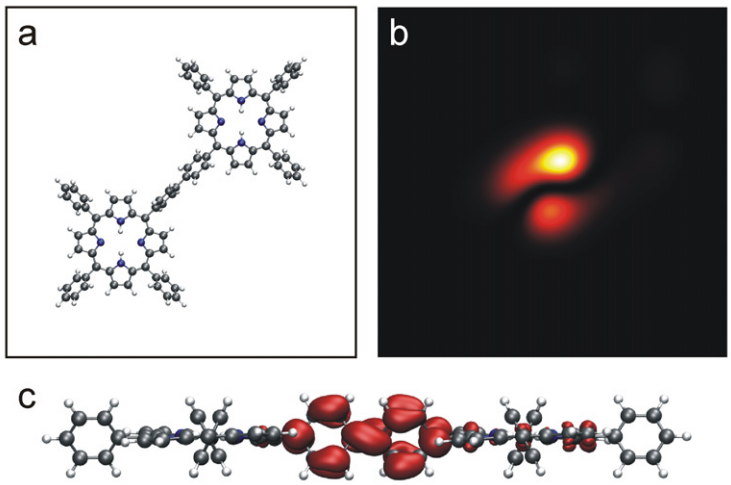

Figure 5.10. (a) Calculated geometric structure of the isolated dimer. The calculated contribution to the local density of states due to the state at about 2.8 eV above the HOMO is shown in (b) at a vertical distance of 7 Å from the porphyrin plane (i.e. a typical tip–surface distance). (a) and (b) correspond to the same area, 3.5×3.5 nm^2 in size. (c) A side view of a 3D contour plot of the orbital density of this state at a much higher density. Calculations done by Matthew Dyer and Mats Persson. Reproduced with permission from [123]. Copyright (2007) Nature Publishing Group.

efficiency and yield. While the results obtained so far show that it is possible to switch such molecules when adsorbed on a surface, the role of side groups and substituents is still unclear. For example, molecular donor or acceptor groups should be attached to the central switching unit in order to change the electronic structure. The second topic of interest concentrates on the molecular interaction with its environment. It is clear that the surface is more than just a supporting substrate and plays an important role, either by defining a specific molecular adsorption or growth mode or by its direct interaction with the adsorbed molecular switches, which could hinder or enable the isomerization process. In order to better understand the influence of these properties, a specific type of molecular switch should be studied on different substrates of similar structure or chemical composition, allowing a direct comparison. In such a way, the properties of an 'ideal' surface by means of efficient switching could be determined. The presented results show that the molecular mobility plays an important role, because single molecules are too mobile to be switched. Thus, it would be advantageous to fix the molecules on one side (by interaction with the substrate or other molecules) and keep the other side free (to allow the switching mechanism). A planar configuration should be maintained, because it facilitates conformational analysis with the STM. Finally, the collective switching of the molecules, observed in the presented experiments, needs to be understood more in detail.

The new method of constructing covalently bound molecular networks on a surface offers exciting possibilities for the growth of functionalized nanostructures. In a next step, this method should be extended to other molecular building blocks. It is expected that this technique should be applicable to a variety of molecules, which would prove its versatility. In particular, the use of different arrangements of activated molecular sites could lead to a variety of macromolecular structures. Furthermore, functionalized molecules should be incorporated into such networks, taking an important step towards molecular electronics. These could be for instance the same porphyrin building blocks that have been presented in this work, but equipped with a functional (e.g. magnetic) centre, or molecular switches. In order to understand the versatility of this method for molecular electronics, the charge transfer between the molecular units must be investigated. The precise arrangement of the aromatic units plays an important role in this regard. By using various types of substituent halogen atoms within one molecule, hierarchical growth mechanisms could be studied and applied by activating the different molecular sites one after the other in a controlled way. Finally, it would be interesting to see whether the observed growth mechanism on a surface can be extended to the third dimension by attaching molecular building blocks vertically.

Acknowledgments

I would like to thank Karl-Heinz Rieder, Francesca Moresco, Micol Alemani, Leo Gross, Leif Lafferentz and Ingeborg Stass at the Freie Universität Berlin, Christian Joachim and co-workers at the CEMES-CNRS Toulouse, Matthew Dyer and Mats Persson of the University of Liverpool and Maike Peters and Stefan Hecht of the Humboldt Universität Berlin for the fruitful collaboration and stimulating discussions. Furthermore, I am grateful to Christian Roth for technical assistance and Nacho Pascual for valuable discussions and critical reading of the manuscript.

I am grateful to Charles M Lieber (Harvard University), J Fraser Stoddart (University of California at Los Angeles), Mark A Ratner (Northwestern University), Petra Tegeder (Freie Universität Berlin) and Saw-Wai Hla (Ohio University) for providing figures from their publications.

Financial support from the European Union, through the projects AMMIST and PICO-INSIDE, and the German

Science Foundation (DFG), through SFB 658 and GR 2697/1, is gratefully acknowledged.

References

[1] Feynman R 1959 *Speech at the Annual Meeting of the American Physical Society (29 December 1959)*
[2] Baller M K *et al* 2000 *Ultramicroscopy* **82** 1
[3] Vadgama P and Crump P W 1992 *Analyst* **117** 1657
[4] Wilson S and Howell S 2002 *Biochem. Soc. Trans.* **30** 794
[5] Zheng G, Patolsky F, Cui Y, Wang W U and Lieber C M 2005 *Nat. Biotechnol.* **23** 1294
[6] Haes A J and Duyne R P V 2002 *J. Am. Chem. Soc.* **124** 10596
[7] Stoddart J F 2001 *Acc. Chem. Res.* **34** 410
[8] Browne W R and Feringa B L 2006 *Nat. Nanotechnol.* **1** 25
[9] Balzani V, Credi A, Silvi S and Venturi M 2006 *Chem. Soc. Rev.* **35** 1135
[10] Astumian R D and Hänggi P 2002 *Phys. Today* **55** 33
[11] Condon A 2006 *Nat. Rev. Genet.* **7** 565
[12] Bath J and Turberfield A J 2007 *Nat. Nanotechnol.* **2** 275
[13] Molloy J E and Veigel C 2003 *Science* **300** 2045
[14] Kwon K-Y, Wong K L, Pawin G, Bartels L, Stolbov S and Rahman T S 2005 *Phys. Rev. Lett.* **95** 166101
[15] Wong K L, Pawin G, Kwon K-Y, Lin X, Jiao T, Solanki U, Fawcett R H J, Bartels L, Stolbov S and Rahman T S 2007 *Science* **315** 1391
[16] Falvo M R, Taylor R M, Helser A, Chi V, Brooks F P, Washburn S and Superfine R 1999 *Nature* **397** 236
[17] Joachim C and Gimzewski J K 2001 *Struct. Bonding* **99** 1
[18] Shirai Y *et al* 2006 *J. Am. Chem. Soc.* **128** 4854
[19] Badjic J D, Balzani V, Credi A, Silvi S and Stoddart J F 2004 *Science* **303** 1845
[20] Ashton P R *et al* 1998 *J. Am. Chem. Soc.* **120** 11932
[21] Balzani V, Clemente-Leon M, Credi A, Ferrer B, Venturi M, Flood A H and Stoddart J F 2006 *Proc. Natl Acad. Sci.* **103** 1178
[22] Moore G 1975 *IEDM Tech. Dig.* 11
[23] Packan P A 1999 *Science* **285** 2079
[24] Joachim C, Gimzewski J K and Aviram A 2000 *Nature* **408** 541
[25] Ellenbogen J C and Love J C 2000 *Proc. IEEE* **88** 386
[26] Heath J R and Ratner M A 2003 *Phys. Today* **56** 43
[27] Huang Y, Duan X, Wei Q and Lieber C M 2001 *Science* **291** 630
[28] Service R F 2001 *Science* **293** 782
[29] Aviram A and Ratner M 1974 *Chem. Phys. Lett.* **29** 277
[30] Dorogi M, Gomez J, Osifchin R, Andres R P and Reifenberger R 1995 *Phys. Rev.* B **52** 9071
[31] Metzger R M *et al* 1997 *J. Am. Chem. Soc.* **119** 10455
[32] Zhao J, Zeng C, Cheng X, Wang K, Wang G, Yang J, Hou J G and Zhu Q 2005 *Phys. Rev. Lett.* **95** 045502
[33] Donhauser Z J *et al* 2001 *Science* **292** 2303
[34] Avouris P, Chen Z and Perebeinos V 2007 *Nat. Nanotechnol.* **2** 605
[35] Ebbesen T W, Lezec H J, Hiura H, Bennett J W, Ghaemi H F and Thio T 1996 *Nature* **382** 54
[36] Cao J, Wang Q and Dai H 2005 *Nat. Mater.* **4** 745
[37] Tans S J, Verschueren A R M and Dekker C 1998 *Nature* **393** 49
[38] Magoga M and Joachim C 1997 *Phys. Rev.* B **56** 4722
[39] Lang N D and Avouris P 2001 *Phys. Rev.* B **64** 125323
[40] Nitzan A and Ratner M A 2003 *Science* **300** 1384
[41] Grill L and Moresco F 2006 *J. Phys.: Condens. Matter* **18** S1887
[42] Kushmerick J G 2005 *Mater. Today* **8** 26
[43] Forshaw M, Stadler R, Crawley D and Nikolic K 2004 *Nanotechnology* **15** S220
[44] Rosei F 2004 *J. Phys.: Condens. Matter* **16** S1373
[45] Lehn J-M 2002 *Science* **295** 2400
[46] Hecht S 2003 *Angew. Chem. Int. Edn* **42** 24
[47] Barth J V, Costantini G and Kern K 2005 *Nature* **437** 671
[48] Barth J V, Weckesser J, Lin N, Dmitriev A and Kern K 2003 *Appl. Phys.* A **76** 645
[49] Reed M A, Zhou C, Muller C J, Burgin T P and Tour J M 1997 *Science* **278** 252
[50] Reichert J, Ochs R, Beckmann D, Weber H B, Mayor M and Löhneysen H v 2002 *Phys. Rev. Lett.* **88** 176804
[51] Kergueris C, Bourgoin J-P, Palacin S, Esteve D, Urbina C, Magoga M and Joachim C 1999 *Phys. Rev.* B **59** 12505
[52] Moresco F 2004 *Phys. Rep.* **399** 175
[53] Otero R, Rosei F and Besenbacher F 2006 *Annu. Rev. Phys. Chem.* **57** 497
[54] Stroscio J A and Eigler D M 1991 *Science* **254** 1319
[55] Stipe B C, Rezaei M A and Ho W 1998 *Science* **279** 1907
[56] Lastapis M, Martin M, Riedel D, Hellner L, Comtet G and Dujardin G 2005 *Science* **308** 1000
[57] Stipe B C, Rezaei M A and Ho W 1998 *Phys. Rev. Lett.* **81** 1263
[58] Ho W 2002 *J. Chem. Phys.* **117** 11033
[59] Whitman L J, Stroscio J A, Dragoset R A and Celotta R J 1991 *Science* **251** 1206
[60] Rezaei M A, Stipe B C and Ho W 1999 *J. Chem. Phys.* **110** 4891
[61] Sugimoto Y, Abe M, Hirayama S, Oyabu N, Custance O and Morita S 2005 *Nat. Mater.* **4** 156
[62] Meyer G 1996 *Rev. Sci. Instrum.* **67** 2960
[63] Grill L, Rieder K-H, Moresco F, Stojkovic S, Gourdon A and Joachim C 2006 *Nano Lett.* **6** 2685
[64] Bartels L, Meyer G and Rieder K-H 1997 *Phys. Rev. Lett.* **79** 697
[65] Jung T A, Schlittler R R, Gimzewski J K, Tang H and Joachim C 1996 *Science* **217** 181
[66] Beton P H, Dunn A W and Moriarty P 1995 *Appl. Phys. Lett.* **67** 1075
[67] Eigler D M and Schweizer E K 1990 *Nature* **344** 524
[68] Heinrich A J, Lutz C P, Gupta J A and Eigler D M 2002 *Science* **298** 1381
[69] Gross L, Rieder K-H, Moresco F, Stojkovic S M, Gourdon A and Joachim C 2005 *Nat. Mater.* **4** 892
[70] Moresco F, Meyer G, Rieder K-H, Tang H, Gourdon A and Joachim C 2001 *Phys. Rev. Lett.* **87** 088302
[71] Moresco F, Meyer G, Rieder K-H, Tang H, Gourdon A and Joachim C 2001 *Appl. Phys. Lett.* **78** 306
[72] Hla S-W, Braun K-F and Rieder K-H 2003 *Phys. Rev.* B **67** 201402
[73] Bouju X, Joachim C and Girard C 1999 *Phys. Rev.* B **59** R7845
[74] Bouju X, Joachim C, Girard C and Tang H 2001 *Phys. Rev.* B **63** 085415
[75] Alemani M, Gross L, Moresco F, Rieder K-H, Wang C, Bouju X, Gourdon A and Joachim C 2005 *Chem. Phys. Lett.* **402** 180
[76] Grill L, Rieder K-H, Moresco F, Stojkovic S, Gourdon A and Joachim C 2005 *Nano Lett.* **5** 859
[77] Keeling D L, Humphry M J, Fawcett R H J, Beton P H, Hobbs C and Kantorovich L 2005 *Phys. Rev. Lett.* **94** 146104
[78] Grill L, Rieder K-H, Moresco F, Rapenne G, Stojkovic S, Bouju X and Joachim C 2007 *Nat. Nanotechnol.* **2** 95
[79] Gimzewski J K, Joachim C, Schlittler R R, Langlais V, Tang H and Johannsen I 1998 *Science* **281** 531
[80] Chiaravalloti F, Gross L, Rieder K-H, Stojkovic S M, Gourdon A, Joachim C and Moresco F 2007 *Nat. Mater.* **6** 30
[81] Shirai Y, Osgood A J, Zhao Y, Kelly K F and Tour J M 2005 *Nano Lett.* **5** 2330

[82] Grill L, Rieder K-H, Moresco F, Jimenez-Bueno G, Wang C, Rapenne G and Joachim C 2005 *Surf. Sci.* **584** L153
[83] Hla S-W 2007 *Nat. Nanotechnol.* **2** 82
[84] Gimzewski J K and Joachim C 1999 *Science* **283** 1683
[85] Iancu V and Hla S-W 2006 *Proc. Natl Acad. Sci.* **103** 13718
[86] Moresco F, Meyer G, Rieder K-H, Tang H, Gourdon A and Joachim C 2001 *Phys. Rev. Lett.* **86** 672
[87] Liljeroth P, Repp J and Meyer G 2007 *Science* **317** 1203
[88] Feringa B L 2001 *Molecular Switches* (Weinheim: Wiley–VCH)
[89] Rando R R 1990 *Angew. Chem. Int. Edn* **29** 461
[90] Rau H 2003 *Photochromism—Molecules and Systems* (Amsterdam: Elsevier)
[91] Nägele T, Hoche R, Zinth W and Wachtveitl J 1997 *Chem. Phys. Lett.* **272** 489
[92] Hugel T, Holland N B, Cattani A, Moroder L, Seitz M and Gaub H 2002 *Science* **296** 1103
[93] Ishikawa T, Noro T and Shoda T 2001 *J. Chem. Phys.* **115** 7503
[94] Zhang C, Du M-H, Cheng H-P, Zhang X-G, Roitberg A E and Krause J L 2004 *Phys. Rev. Lett.* **92** 158301
[95] Kirakosian A, Comstock M J, Cho J and Crommie M F 2005 *Phys. Rev.* B **71** 113409
[96] Miwa J A, Weigelt S, Gersen H, Besembacher F, Rosei F and Linderoth T 2006 *J. Am. Chem. Soc.* **128** 3164
[97] Comstock M J *et al* 2007 *Phys. Rev. Lett.* **99** 038301
[98] Comstock M J, Cho J, Kirakosian A and Crommie M F 2005 *Phys. Rev.* B **72** 153414
[99] Choi B Y, Kahng S J, Kim S, Kim H, Kim H W, Song Y J, Ihm J and Kuk Y 2006 *Phys. Rev. Lett.* **96** 156106
[100] Henzl J, Mehlhorn M, Gawronski H, Rieder K H and Moregnstern K 2006 *Angew. Chem. Int. Edn* **45** 603
[101] Alemani M, Peters M V, Hecht S, Rieder K-H, Moresco F and Grill L 2006 *J. Am. Chem. Soc.* **128** 14446
[102] Forber C L, Kelusky E C, Bunce N J and Zerner M C 1985 *J. Am. Chem. Soc.* **107** 5884
[103] Ishikawa T, Noro T and Shoda T 2001 *J. Chem. Phys.* **115** 7503
[104] Neta P and Levanon H 1977 *J. Phys. Chem.* **81** 2288
[105] Olesen L, Brandbyge M, Sorensen M R, Jacobsen K W, Laegsgaard E, Stensgaard I and Besenbacher F 1996 *Phys. Rev. Lett.* **76** 1485
[106] Füchsel G, Klamroth T, Dokic J and Saalfrank P 2006 *J. Phys. Chem.* B **110** 16337
[107] Saalfrank P 2000 *J. Chem. Phys.* **113** 3780
[108] Hagen S, Leyssner F, Nandi D, Wolf M and Tegeder P 2007 *Chem. Phys. Lett.* **444** 85
[109] Tegeder P, Hagen S, Leyssner F, Peters M V, Hecht S, Klamroth T, Saalfrank P and Wolf M 2007 *Appl. Phys.* A **88** 465
[110] Whitesides G M and Grzybowski B 2002 *Science* **295** 2418
[111] Theobald J A, Oxtoby N S, Phillips M A, Champness N R and Beton P H 2003 *Nature* **424** 1029
[112] Pawin G, Wong K L, Kwon K-Y and Bartels L 2006 *Science* **313** 961
[113] Hameren R V *et al* 2006 *Science* **314** 1433
[114] Stöhr M, Wahl M, Galka C H, Riehm T, Jung T A and Gade L H 2005 *Angew. Chem. Int. Edn* **44** 7394
[115] Keeling D L, Oxtoby N S, Wilson C, Humphry M J, Champness N R and Beton P H 2003 *Nano Lett.* **3** 9
[116] Yokoyama T, Yokoyama S, Kamikado T, Okuno Y and Mashiko S 2001 *Nature* **413** 619
[117] Rabe J P and Buchholz S 1991 *Science* **253** 424
[118] Lin N, Dmitriev A, Weckesser J, Barth J V and Kern K 2002 *Angew. Chem. Int. Edn* **41** 4779
[119] Cote A P, Benin A I, Ockwig N W, O'Keeffe M, Matzger A J and Yaghi O M 2005 *Science* **310** 1166
[120] Zambelli T *et al* 2004 *Int. J. Nanosci.* **3** 331
[121] Hla S-W, Bartels L, Meyer G and Rieder K-H 2000 *Phys. Rev. Lett.* **85** 2777
[122] Hahn J R and Ho W 2001 *Phys. Rev. Lett.* **87** 166102
[123] Grill L, Dyer M, Lafferentz L, Persson M, Peters M V and Hecht S 2007 *Nat. Nanotechnol.* **2** 687
[124] Hla S-W, Meyer G and Rieder K-H 2003 *Chem. Phys. Lett.* **370** 431
[125] Spillmann H, Kiebele A, Stöhr M, Jung T A, Bonifazi D, Cheng F and Diederich F 2006 *Adv. Mater.* **18** 275
[126] McCarty G S and Weiss P S 2004 *J. Am. Chem. Soc.* **126** 16772
[127] Anderson H L 1999 *Chem. Commun.* 2323